Origin of the fast magnetic relaxation close to T_c in $YBa_2Cu_3O_{7-\delta}$

I. Isaac and J. Jung
Department of Physics, University of Alberta, Edmonton, Alberta, Canada T6G 2J1
(Received 9 October 1996)

There have been many reports on magnetization measurements of the normalized logarithmic decay rate $S(T,H)$, which was observed to increase rapidly with temperature T close to T_c in $YBa_2Cu_3O_{7-\delta}$ (YBCO) single crystals, epitaxial thin films, and granular bulk samples (grain aligned and with random orientation of the grains). We investigated the origin of $S(T,H)$ by performing the following measurements: (1) the relaxation of the persistent current from its critical value, as a function of temperature T and magnetic field H; (2) the temperature dependence of the critical current at different magnetic fields. The measurements were carried out on granular YBCO and RBCO (where R stands for rare-earth elements) ring-shaped samples with randomly oriented grains, which always exhibit an increase of $S(T,H)$ with temperature close to T_c. The results revealed the correlation between the temperature dependence of the unperturbed pinning potential, $U_0 = kT/S$, and that of the critical current. Such correlation suggests that variations of the Josephson coupling energy, or the order parameter, along the grain boundaries are responsible for weak flux pinning and consequently the increase of S close to T_c. The analysis of these results was made using the Tinkham-Lobb [Solid State Phys. **42**, 91 (1989)] model of flux pinning in a granular superconductor and their description of the conceptual equivalence between the weak-link (Ambegaokar-Baratoff) and continuum (Ginzburg-Landau) flux-pinning models. According to the results of these studies, we conclude that the divergence of $S(T,H)$ close to T_c observed in YBCO single crystals and epitaxial thin films could stem from filamentary superconducting structures caused, for instance, by phase separation. [S0163-1829(97)07513-9]

I. INTRODUCTION

The magnitude of the effective critical current density J_c in high-temperature superconductors is limited by the magnetic-flux-induced rapid decay of the current. Large thermal fluctuations at high operating temperatures, combined with the small flux pinning energy barrier, are believed to be responsible for this process.[1] Another factor which limits J_c is the sample's granularity caused by the presence of the grain boundaries, twin boundaries, or phase separation.[2] In this case the magnitude of the sample's critical current is restricted by the decoupling critical current of the Josephson tunnel or proximity junctions and the critical current of the intergrain microbridges.

Evaluation of the relaxation rate of the persistent current has been usually carried out by measuring the sample's magnetization M as a function of time t for different temperatures T and magnetic fields H. There have been many reports of the fast normalized decay rate S in $YBa_2Cu_3O_{7-\delta}$ (YBCO), defined as $(1/M_0)(dM/d\ \ln t)$, whose value increases dramatically with temperature close to T_c. The rise of $S(T,H)$ close to T_c has been observed in YBCO single crystals (both as grown and irradiated), epitaxial thin films, and grain-aligned melt-textured samples as well as in granular ceramic YBCO.[3–14]

The available results for single crystals are those of Yeshurun *et al.*,[3] Brawner *et al.*,[4] Civale *et al.*,[5] and Thompson *et al.*[6] They were obtained using either a superconducting quantum interference device (SQUID) magnetometer[3,5,6] or a Hall probe.[4] Yeshurun *et al.*[3] measured the magnetic relaxation versus temperature in YBCO crystals after applying a field of 600 G (parallel to the c axis) to the zero-field-cooled sample. Their data were analyzed by Hagen and Griessen[7] who produced the $S(T,H)$ curve over a temperature range of 5–70 K with S monotonically increasing with temperature above 20 K. Brawner *et al.*[4] performed precision measurements of the relaxation of the remanent magnetization in YBCO single crystals over a temperature range of 2–70 K. The remanent magnetization was achieved by applying and subsequently switching off an external field of 6 T. The results show a sharp jump in $S(T)$ at temperatures above 40 K. Civale *et al.*[5] and Thompson *et al.*[6] published the magnetic relaxation data for proton-irradiated single crystals over a temperature range of 4–80 K and in a field of 1 T parallel to the c axis. The results of Civale *et al.* show an increase of normalized decay rate S with temperature above 60 K and those of Thompson *et al.* at temperatures above 40 K.

Goodyear *et al.*[8] reported a divergence in the relaxation rate S close to T_c on over 300 epitaxial YBCO thin films. They measured the remanent magnetic relaxation, using a Hall probe, in zero-field-cooled films after application of a short magnetic field pulse sufficiently large (20–300 G parallel to the c axis) to place the film in the critical state. An increase in S with temperature above 70–80 K was consistently found in all square-shaped and patterned ring-shaped thin films. Darhmaoui *et al.*[9] studied the logarithmic relaxation of the self-field of persistent current circulating in a ring-shaped YBCO thin film with T_c $(R=0)$ of 81 K. Measurement of the time decay of the persistent current from its critical level was done on a zero-field-cooled ring using a Hall probe. $S(T,H)$ for this film increases with temperature at temperatures above 60 K. Enpuku *et al.*[10] derived the temperature dependence of the pinning potential $U_0(T)$ from the temperature dependence of the current-voltage I-V characteristics of YBCO thin films. $U_0(T)$ was calculated from the slope of $\ln V$ vs $(1/T)$ curves according to the conventional

flux creep model of Anderson and Kim. $U_0(T)$ decreases with an increasing temperature at temperatures above 50 K, implying an increase in $S(T)=kT/U_0(T)$.

Some melt-processed grain-aligned YBCO bulk samples are known to attain higher values of $S(T,H)$ close to T_c. This was shown by Welch[11] who reported an increase of S obtained from the magnetization relaxation (SQUID) measurements in the presence of magnetic fields of 1–4 T and by Keller *et al.*[12] who obtained S from the time decay of the remanent moment in the full critical state using a vibrating-sample magnetometer.

A rise of $S(T,H)$ close to T_c was shown to occur in randomly oriented polycrystalline (ceramic) YBCO by Mee *et al.*[13] and Jung *et al.*[14] Mee *et al.* studied relaxation of persistent current in YBCO rings of very low critical current density. A measurement was performed on a zero-field-cooled ring, after a field as low as 0.1 G was applied to the sample and subsequently removed. The resulting magnetic field at a point near the center of the ring was measured using a conventional niobium rf SQUID connected via a superconducting flux transformer. An increase of $S(T,H)$ at temperatures above 40 K was recorded. Jung *et al.* reported a jump in $S(T)$ above 80 K for a zero-field-cooled ceramic composite of YBCO/Ag (2 wt. %). They used a Hall probe to detect logarithmic relaxation of persistent current induced in a ring-shaped sample of this composite. Critical persistent current was generated by applying and subsequently reducing to zero an external magnetic fields as low as 20 G.

Paulius *et al.*[15] observed an increase in the decay rate S with increasing temperature close to T_c in the $(Pr_xY_{1-x})Ba_2Cu_3O_{7-\delta}$ system for $0\leqslant x\leqslant 0.4$. They measured magnetic relaxation on zero-field-cooled samples in a magnetic field of 0.5 T using a SQUID magnetometer. A rise of $S(T)$ was recorded close to T_c for all substitution levels.

The results quoted above suggest that the fast normalized relaxation rate S close to T_c is a feature which is independent of the type of YBCO material, the sample geometry, or the relaxation measurement technique. However, little was known about the origin of this fast relaxation process, including the character of vortices which are responsible for the dissipation of supercurrents close to T_c. Kung *et al.*[16] suggested that the behavior of $S(T)$ depends on the type of pinning centers (e.g., defects such as stacking faults and twin boundaries) and compositional inhomogeneity (e.g., minority phases). They stated that for measurements taken only at lower temperatures the divergence of $S(T)$ close to T_c will be missed, leading to the wrong or incomplete conclusions for the temperature dependence of the normalized relaxation rate at high temperatures. Paulius *et al.*,[15] on the other hand, suggested that an increase of $S(T)$ could be a reflection of the softening of the flux lattice on approaching the melting line.

The objective of this work was to study and to explain the phenomena that cause an increase of S at temperatures close to T_c. We decided to investigate $S(T,H)$ in ceramic polycrystalline samples rather than in single crystals or epitaxial thin films. The reasons for this are the following.

(i) Magnetic moments measured in tiny single crystals and thin films are very small close to T_c, thereby reducing dramatically the accuracy of the relaxation measurements.

(ii) The magnetic response can be enhanced in measurements on bulk ceramic samples, where the total critical current can be increased by increasing the sample's cross-sectional area, thus allowing detection of dissipation very close to T_c.

(iii) Our studies have pointed out that *all* ceramic samples of YBCO or *R*BCO (where *R* stands for rare-earth elements), which exhibit flux-creep-induced dissipation, are characterized by the increase of S with temperature close to T_c.

Measurements of $S(T,H)$ were performed by the detection of decay of a self-supporting (persistent) critical current induced in a ring shaped sample. A Hall probe was used to record changes in a magnetic field produced by the current. The advantages of this technique are the following.

(i) The temperature and magnetic field dependence of the critical current $I_c(T,H)$ and that of $S(T,H)$ can be obtained during the same experiment.

(ii) The method allows one to distinguish depairing critical current from depinning one and to compare their dependence on temperature.

In this paper we present experimental results for $S(T,H)$ in granular (ceramic) YBCO and *R*BCO samples over a temperature and magnetic field range of 65–95 K and 0–100 G, respectively. The experiments were performed for $YBa_2Cu_3O_{7-\delta}$, $YBa_2Cu_3O_{7-\delta}$/Ag(x wt. %) (YBCO/Ag x wt. %) composites (where $x=2$ and 4), and rare-earth-element-substituted samples such as $GdBa_2Cu_3O_{7-\delta}$ (GBCO), $EuBa_2Cu_3O_{7-\delta}$ (EBCO), and $(Pr_xY_{1-x})Ba_2Cu_3O_{7-\delta}$ (PYBCO) with $x=0.15$ and 0.20. This set of samples allowed us to investigate $S(T,H)$ in materials of different T_c, different $J_c(T)$, and different flux pinning strengths.

We measured (1) the logarithmic time decays of the persistent current for different temperatures between 65 and 95 K for zero-field cooling and field cooling (over a magnetic field range 10–60 G) in order to determine variation of the pinning potential $U_0(T,H)=kT/S(T,H)$ with temperature and magnetic field; (2) the temperature dependence of the critical persistent current for zero-field cooling and field cooling conditions. We found a correlation between the temperature dependence of the pinning potential and that of the critical current. This correlation was discussed using the model of granular superconductivity developed by Tinkham and Lobb.[17]

II. EXPERIMENTAL PROCEDURE

A. Description of the measurement method

Critical currents and their decay were investigated using ring-shaped samples and an axial scanning Hall probe. A self-supporting (persistent) current was induced in the ring by applying and subsequently removing an external magnetic field in the direction perpendicular to the ring's plane, using a nonsuperconducting solenoid. The profile of the axial component of the magnetic field generated by the persistent current across the ring was recorded using a scanning Hall probe. The magnitude of the critical current was inferred from the maximum self-field of the persistent current at the ring's center using the Biot-Savart law. The decay rate of the persistent current from its critical value was deduced from the relaxation of the persistent current's self-field. This method eliminated the contribution of normal currents to the

measured value of the critical current and allowed us to distinguish between depairing critical currents (which do not exhibit time decay) and depinning ones (whose magnitude decays with time). Measurements of the critical current and its decay were performed in the absence and in the presence of an external applied magnetic field using zero-field-cooling (ZFC) and field-cooling (FC) procedures, respectively. In the ZFC case, a bell-shaped profile of the persistent current's self-field was recorded by an axial Hall probe after an external field H was applied and subsequently removed. By increasing the magnitude of H, it was possible to generate larger persistent currents of magnitudes up to a critical value. The critical state was determined by detecting the saturation of the persistent current's self-field with an increasing H. In the FC case, on the other hand, the ring was cooled below T_c in the presence of a constant external field H in the direction perpendicular to the ring's plane. At the ring's center, the magnetic field was recorded to be $H-H_M$, where H_M is the Meissner field. Then an additional field $H_{\rm ad}$ was applied and subsequently reduced to zero, in order to induce a persistent current at H, using a procedure similar to that in the ZFC case. The critical persistent current at H was generated when the persistent current's self-field reached saturation with an increasing $H_{\rm ad}$. For both ZFC and FC cases, the critical current I_c was determined from the Biot-Savart law, using the saturation value of the axial component of the persistent current's self-field at the center of the ring.

The rings studied here had the outer and inner diameters of 15–16 and 6 mm, respectively, and were 3–3.5 mm thick. A 3.5-mm-deep notches were cut along the ring's diameter, forming bridges of width 1–1.5 mm close to the inner hole in order to reduce the ring's cross-sectional area available for the current and to force the current to circulate around the inner hole of the ring. The notches also allowed us to generate the persistent current using low applied fields and to avoid unwanted contribution of the intragrain flux to the self-field of the current. The profiles of the persistent current's self-field were scanned over a distance of 22 mm and at a height of 2 mm with a Hall probe of the sensitive area of 0.4 mm^2 and with a sensitivity of 20–30 mG. The profiles were found to be independent of the scanning direction (parallel or perpendicular to the notches). More details of this experimental technique have been published earlier.[14,18]

B. Sample preparation

Polycrystalline ceramic samples of YBCO, YBCO/Ag, and *R*BCO were prepared using the standard solid-state reaction method, from high-purity (99.999%) oxides and carbonates. The general procedure included pressing a mixture of powders (using 2.5–2.7 kbar of pressure) in order to form disks with diameter of 16 mm. This was followed by calcining the samples in air or flowing oxygen for 24 h at $T_{\rm cal}$=925–950 °C. The resulting product was pulverized and new disk-shaped pellets, 16 mm in diameter and 3 mm thick, were formed under a pressure of 6.2 kbar. The disks were sintered in flowing oxygen at $T_{\rm sin}$=920–930 °C for 7 h and cooled at variable rates down to room temperature (3 °C/min between $T_{\rm sin}$ and 700 °C and 1 °C/min below 700 °C).

YBCO sample No. 1 was produced at $T_{\rm cal}$=925 °C and $T_{\rm sin}$=925 °C using flowing oxygen during calcining. YBCO sample Nos. 2 and 3 were calcined at $T_{\rm cal}$=950 °C in air and sintered twice at $T_{\rm sin}$=930 °C. By varying the calcining and sintering conditions, we were able to produce ceramics of low and high intergrain critical current density and similar intragrain T_c of the order of 90–91 K.

YBCO/Ag composites with 2 and 4 wt. % of Ag were prepared by adding silver to YBCO (which was calcined at $T_{\rm cal}$=925 °C) before a single sintering process at $T_{\rm sin}$=925 °C in flowing oxygen.

*R*BCO compounds [$GdBa_2Cu_3O_{7-\delta}$ (GBCO) and $EuBa_2Cu_3O_{7-\delta}$ (EBCO)] were calcined at $T_{\rm cal}$=950 °C in air and sintered at $T_{\rm sin}$=920 °C in flowing oxygen.

$Pr_{0.15}Y_{0.85}Ba_2Cu_3O_{7-\delta}$ [$(Pr_{0.15}Y_{0.85})$BCO] and $Pr_{0.2}Y_{0.8}Ba_2Cu_3O_{7-\delta}$ [$(Pr_{0.2}Y_{0.8})$BCO] were manufactured by replacing the proper portion of Y_2O_3 with Pr_6O_{11} oxide. The powder was calcined at $T_{\rm cal}$=905 °C for a total time of 137 h. The powder was recrushed and annealed 3 times during this process, and then sintered in a disk form in flowing oxygen at $T_{\rm sin}$=920 °C.

After sintering, a 6-mm-diam hole was cut in the disk center with a diamond tube-shaped drill sprayed with water. The resulting ring was then cut along its diameter in order to form two bridges of width 1.0–1.5 mm close to the hole.

III. EXPERIMENTAL RESULTS

We measured the temperature dependence of the critical current I_c over a temperature range 64–95 K in the absence of the external magnetic field [zero-field-cooling (ZFC) case] and in the presence of a constant field [field-cooling (FC) case] between 10 and 60 G. Figure 1 shows the results of these measurements for nine different granular ring-shaped samples. The Hall probe used in these measurements could detect magnetic fields generated by the persistent currents of magnitude larger than about 10–20 mA. This condition therefore sets the criterion for the ''zero-resistance'' T_c^* of the intergrain junction which is less than the intragrain T_c. External magnetic fields cause a gradual reduction of T_c^*. External fields also are responsible for changes in $I_c(T)$ close to T_c for YBCO and *R*BCO samples from linear behavior to a ''concave'' Ginzburg-Landau-like one.

Measurement of the dependence of the critical persistent current on time revealed that the investigated samples belong to two different groups which are characterized by either the absence of the time decay of the persistent current's self-field (depairing critical current) or the presence of the decay (depinning critical current). In the former case no decay criterion was determined by the sensitivity limit of the Hall probe. The Hall probe could not detect changes in the persistent current less than about 10 mA per decade. Figures 1(a), 1(b), and 1(c) present $I_c(T,H)$ for the depairing critical current. No dissipation of the critical current was recorded for both ZFC and FC cases. In the latter case (depinning critical current), the decay of the persistent current's self-field was observed for the whole temperature range of 64–95 K and for both ZFC and FC cases. Figures 1(d)–1(i) show $I_c(T,H)$ for the depinning critical currents.

The experimental data revealed that the temperature dependence of the critical current is independent of the process of the current dissipation. This can be seen in Fig. 1. The temperature dependence of the depairing critical current shown in Figs. 1(a), 1(b), and 1(c) is very similar to that for

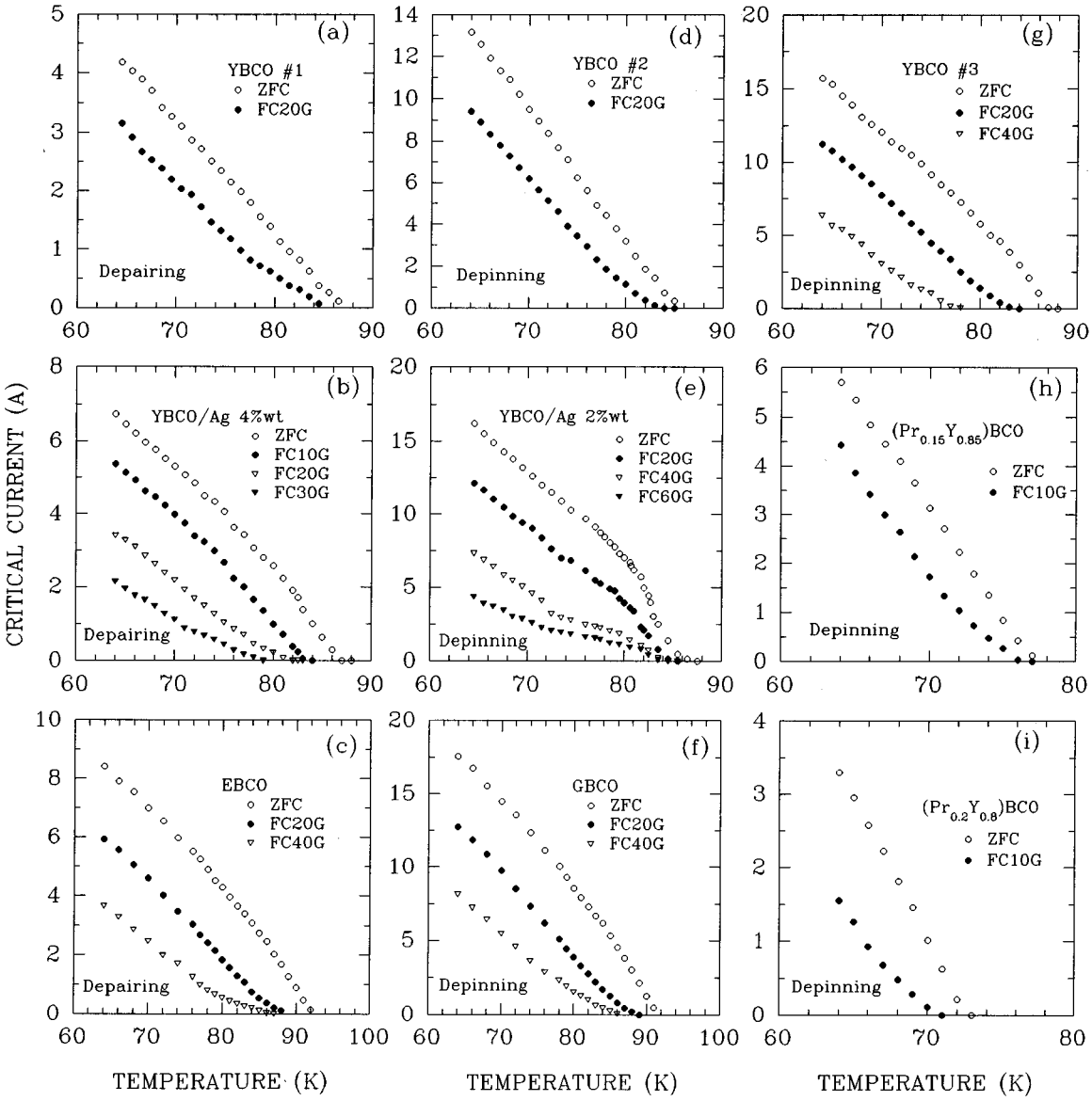

FIG. 1. Temperature dependence of the critical current I_c close to T_c in granular (ceramic) YBCO and RBCO (R=Eu, Gd, and Pr) samples measured at different magnetic fields. (a), (b), and (c) present the depairing critical currents; (d)–(i) show the results for the depinning critical currents. Note the similarities between the temperature dependence of the depairing critical currents and that of the depinning ones exhibited by (a) and (d) for YBCO, (b) and (e) for YBCO/Ag, and (c) and (f) for EBCO and GBCO.

the depinning critical current in Figs. 1(d), 1(e), and 1(f), respectively.

The decay of the persistent current from its critical value was measured for all the depinning critical current cases for both zero-field-cooling and field-cooling procedures. We found that the current decays logarithmically with time over the waiting time range of 10–20 000 sec. The logarithmic behavior dominates the decay process for all the sample studied. Therefore we decided to calculate the normalized logarithmic decay rate S from shorter decay measurements, which lasted up to 1000 sec. Figure 2 shows the temperature dependence of S for six samples of YBCO, YBCO/Ag, and RBCO. For both ZFC and FC cases, decay rates increase with temperature reaching high values near T_c^*. Diverging behavior of S close to T_c is the same for all the investigated compounds, and it is independent of T_c^* or the applied field. S is also independent of the position of the Hall probe along the ring's diameter.

IV. DISCUSSION

In order to generate a circulating persistent current in the zero-field-cooled granular ring-shaped superconductor, we applied an external magnetic field H in the direction perpendicular to the plane of the ring. At H equal to the intergranular critical field H_{c1J}, the magnetic field enters the bulk of the ring through high-angle grain boundaries. During the process of flux penetration into the hole of the ring, some magnetic flux is trapped by the grain boundaries in the form of intergranular vortices. When the applied field H is removed, persistent current is induced and the intergranular vortices remain trapped in the structure of intergranular weak

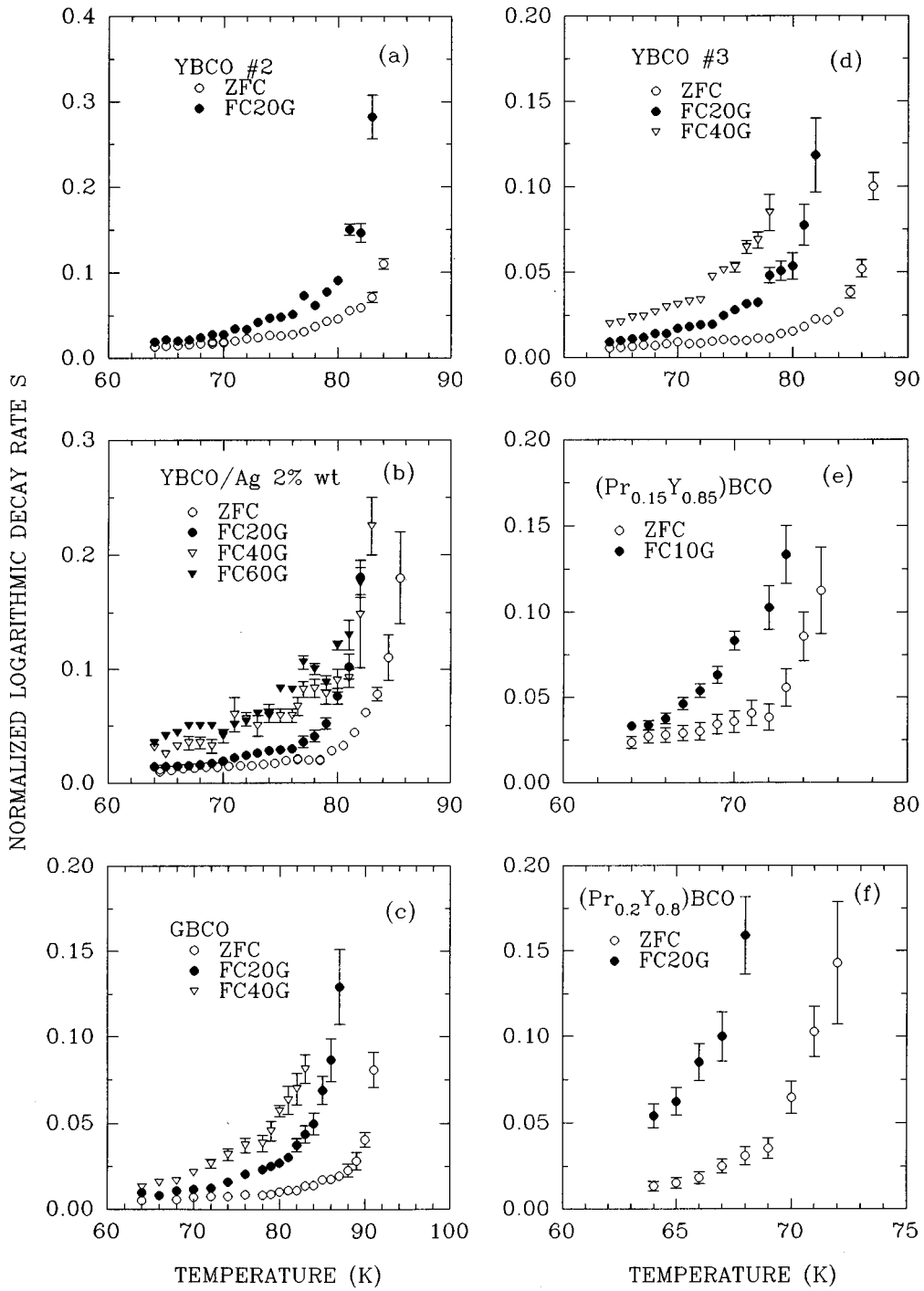

FIG. 2. Temperature dependence of the normalized decay rate S close to T_c for the depinning critical currents in six different samples of YBCO and RBCO (R=Gd and Pr). Note that the magnitude of S at constant temperature increases with the applied magnetic field.

links. Persistent current exerts the Lorentz force on these vortices and, thereby, reduces their effective pinning potential for thermally activated motion in the radial direction away from the center of the ring. This process drains energy from the current and causes its dissipation. The maximum dissipation is expected when the persistent current reaches its critical value.

Tinkham and Lobb[17] described the process of dissipation of the current circulating in a simple granular ring (of inductance L) which contains a large number of weak links in series, with total normal resistance R_n. They assumed that in the superconducting state the resistance is reduced to a value R. Here R varies exponentially with the current I, roughly as $\exp(hI/4ekT)$, taking into account the results of the Ambegaokar-Halperin model of the I-V relation of a highly damped junction, with the normalized barrier height $\gamma_0=2E_J/kT$ as a parameter. Tinkham and Lobb identified the Josephson barrier energy $2E_J$ with the activation energy (the unperturbed pinning potential) U_0, so that the Ambegaokar-Halperin parameter γ_0 is modified to $\gamma_0=U_0/kT$. This was

possible because of the conceptual equivalence between the weak link and continuum flux pinning models. They made the approximation that R varies with the normalized current $i=I/I_c$ according to the equation

$$R=R_n\exp[-\gamma_0(1-i)]. \tag{1}$$

For $I=I_c$, R reduces to R_n.

When the persistent current I is established in the ring, the induced and resistive voltages are balanced. This results in the equation

$$-LdI/dt=IR=IR_n\exp[-\gamma_0(1-i)]. \tag{2}$$

This equation governs the decay of the current. Its solution was obtained with simplifying approximation that the decrease in I is small. Integration of Eq. (2) with the initial condition $I=I_c$ at $t=0$ gives

$$i=1-(1/\gamma_0)\ln(1+\gamma_0 t/\tau_n), \tag{3}$$

with $\tau_n=L/R_n$ as a time constant.

For $\gamma_0\gg 1$, Eq. (3) reduces to

$$di/d\ \ln t=-1/\gamma_0=-kT/U_0 \tag{4}$$

or

$$S=-kT/U_0, \tag{5}$$

where $S=(1/I_c)(dI/d\ \ln dt)$ is the normalized logarithmic decay rate. Equation (5) can be used to calculate $U_0(T)$, the unperturbed pinning potential, if the normalized logarithmic decay rate S is known.

The Tinkham-Lobb model provides a clear description of the relaxation processes that take place in our granular rings, where the logarithmic ''steady-state'' relaxation of the current from the critical level starts about 10 sec after the critical current was established. This behavior is in contrast with that exhibited by some grain-aligned YBCO samples with low-angle grain boundaries (see, e.g., Ref. 18). In these samples the steady-state logarithmic relaxation originates after waiting approximately 1000 sec, and the normalized logarithmic decay rate S does not change with temperature close to T_c.

Tinkham and Lobb analyzed the origin of the intergrain vortex pinning in granular high-temperature superconductors using a highly simplified discrete model of grains of an ideal crystalline superconductor connected by weak links. Each link was characterized by the Josephson coupling energy E_J which is proportional to the link's critical current I_c. Two different pinning regimes were considered: (1) pinning due to the existence of discreteness in the model and (2) pinning due to random variation of E_J in the system.

The first regime was studied by Lobb *et al.*[19] for a square and triangular arrays. They suggested that a Josephson vortex must overcome an energy barrier in order to move from one position to an equivalent neighboring position (see Fig. 1 in Ref. 19). Calculations showed that this energy barrier has a maximum value of $0.2E_J$ for a square array and $0.043E_J$ for a triangular lattice. The basic core energy of an isolated vortex in a two-dimensional square lattice in zero field was computed by Tinkham *et al.*,[20] giving the value of $4E_J$. The energy barrier of $0.2E_J$ is only 5% of the above value.

The second regime was discussed by Tinkham *et al.*[20] It was attributed to the presence of large-scale inhomogeneities which stem from compositional variations, second phases, grain boundaries, twin boundaries, dislocations, etc. Within the discrete model, these inhomogeneities cause E_J to have a range of various values in the different weak links. Also, they introduce geometrical irregularities in the coordination number. These factors affect the core energy of a vortex. Variation in the core energy in different vortex sites and in the magnitude of E_J provides the pinning energy $U_0\sim\delta(4E_J)$ for the vortex.

Tinkham and Lobb suggested the conceptual equivalence between the pinning in the weak-link and continuum models with inhomogeneities. In the granular view the pinning arises because of the variations of E_J from link to link. In the conventional (Ginzburg-Landau) continuum pinning view, on the other hand, the vortex pinning energy results from variations of the order parameter from point to point. In both cases the depth of modulation comes from the degree of disorder in the material. The energy scale is the same in both points of view. Using the Ginzburg-Landau expression for the critical current density, the Josephson coupling energy is $E_J=(H_c^2/8\pi)(4\pi\xi^3)(\pi/2\sqrt{3})$, where H_c and ξ are the thermodynamic critical field and the Ginzburg-Landau coherence length, respectively. This energy is, within a small numerical factor, the characteristic Ginzburg-Landau energy $(H_c^2/8\pi)(4\pi\xi^3)[\ln(\lambda/\xi)]$ (where λ is the Ginzburg-Landau penetration depth) associated with a length ξ of a flux line vortex, from which the pinning energies are derived. Thermally activated flux motion is described in terms of a characteristic pinning energy U_0. In the weak-link model U_0 scales with $4E_J$, and in the continuum model U_0 scales with $(H_c^2/8\pi)(4\pi\xi^3)$. In both cases, these energies are reduced in proportion to the fractional modulation of the characteristic energies from point to point.

We calculated $U_0(T,H)$ from the normalized logarithmic decay rates $S(T,H)=kT/U_0(T,H)$ shown in Fig. 2 for six different samples. These results are presented in Figs. 3 and 4 together with the corresponding ones for $I_c(T,H)$. They reveal that U_0 decreases monotonically with an increasing temperature and approaches zero at temperatures close to T_c^*. An external magnetic field H suppresses $U_0(T)$. The dependence of U_0 on temperature and magnetic field resembles that of $I_c(T,H)$.

For all zero-field-cooled samples, except YBCO/Ag (2 wt. %), the temperature dependence of I_c appears to be Ambegaokar-Baratoff (AB) like. The temperature dependence changes to a Ginzburg-Landau (GL) one [where $I_c\propto(T_c-T)^{3/2}$] in the presence of an external magnetic field (the FC case). This is shown clearly in Fig. 5, where $I_c(T)$ is plotted as $I_c^{2/3}$ versus temperature in order to identify the GL portion of the $I_c(T)$ curve. $I_c(T)$ data taken in the absence of an applied field (the ZFC case) demonstrate a crossover from an AB temperature dependence at low temperatures to a GL one at high temperatures very close to T_c. The AB→GL crossover temperature decreases with an increasing external magnetic field. Crossover effects in the temperature dependence of $I_c(T)$ in granular YBCO and epitaxial YBCO thin films were investigated by Darhmaoui and Jung.[21] The AB→GL crossover in $I_c(T)$ was found to be similar in both types of YBCO. According to Clem *et al.*[22] the AB→GL

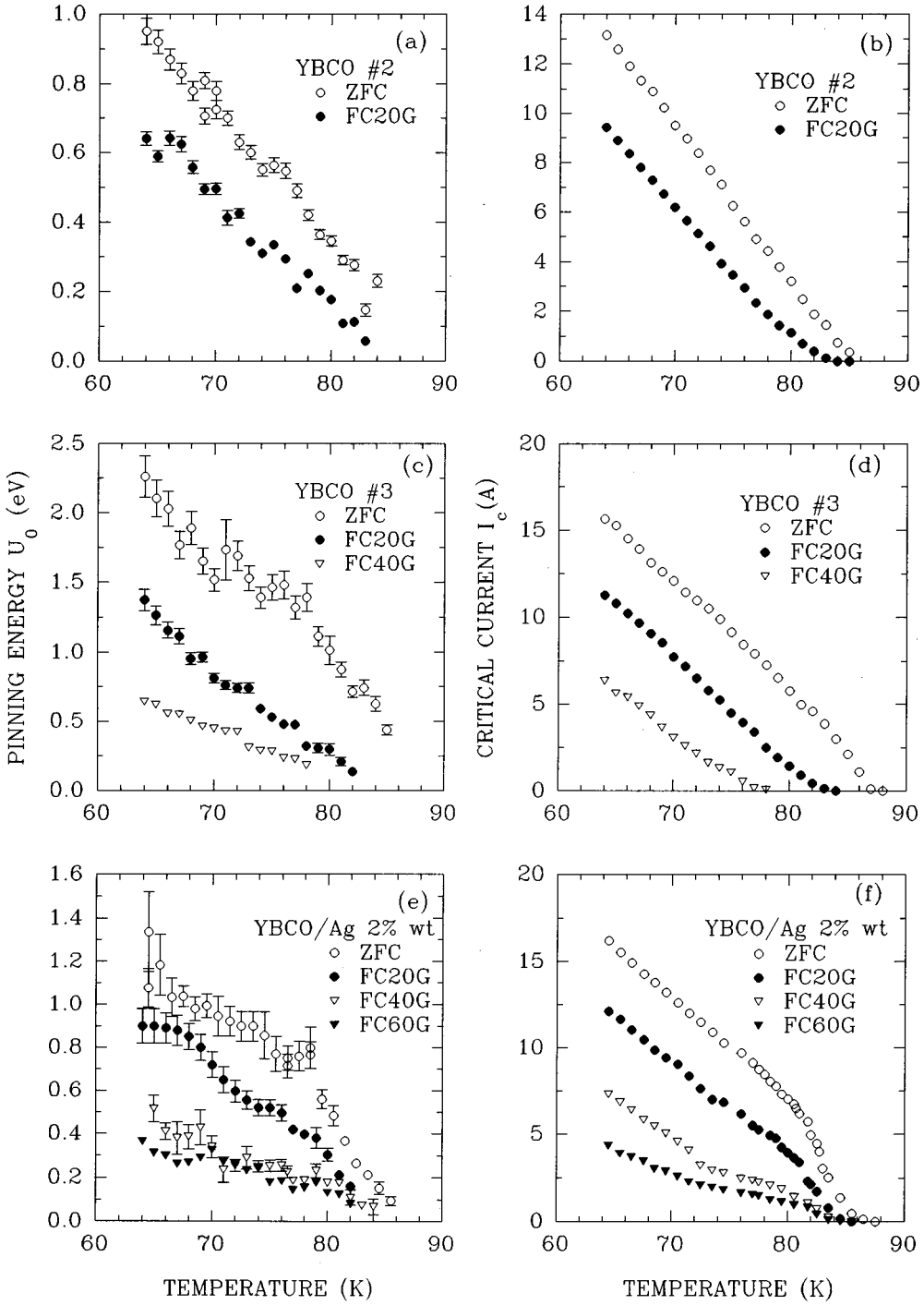

FIG. 3. Comparison of the temperature dependence of the unperturbed pinning potential $U_0(T,H)=kT/S(T,H)$ with that of the critical current $I_c(T,H)$ for granular YBCO and YBCO/Ag samples. Note the similarities between the temperature dependence of $U_0(T,H)$ and that of $I_c(T,H)$.

crossover in $I_c(T)$ is an indication of granularity of a superconductor whose grains are coupled by Josephson tunnel junctions. At the AB→GL crossover temperature, the coherence length $\xi(T)$ equals the grain size a_0. Below the crossover temperature, $I_c(T)$ is governed by Josephson tunnel junctions (AB behavior). Above the crossover temperature, the supercurrent does not ''see'' the junctions and $I_c(T)$ is governed by the ability of the supercurrent to suppress the superconducting gap parameter in the grains (GL behavior). The observation of the AB→GL crossover in $I_c(T)$ of YBCO implies the presence of microdomain structure (superconducting microdomains coupled by Josephson tunnel junctions). In YBCO thin films of $T_c \geqslant 90$ K, the AB→GL crossover temperature is 80–82 K, and therefore the effective size of microdomains $a_0=\xi(80\text{–}82\ \text{K})=30\text{–}40$ Å. The existence of microdomain structure in YBCO was recently confirmed by Etheridge[23] in high-resolution electron microscopy studies. Similarities between the AB→GL crossover

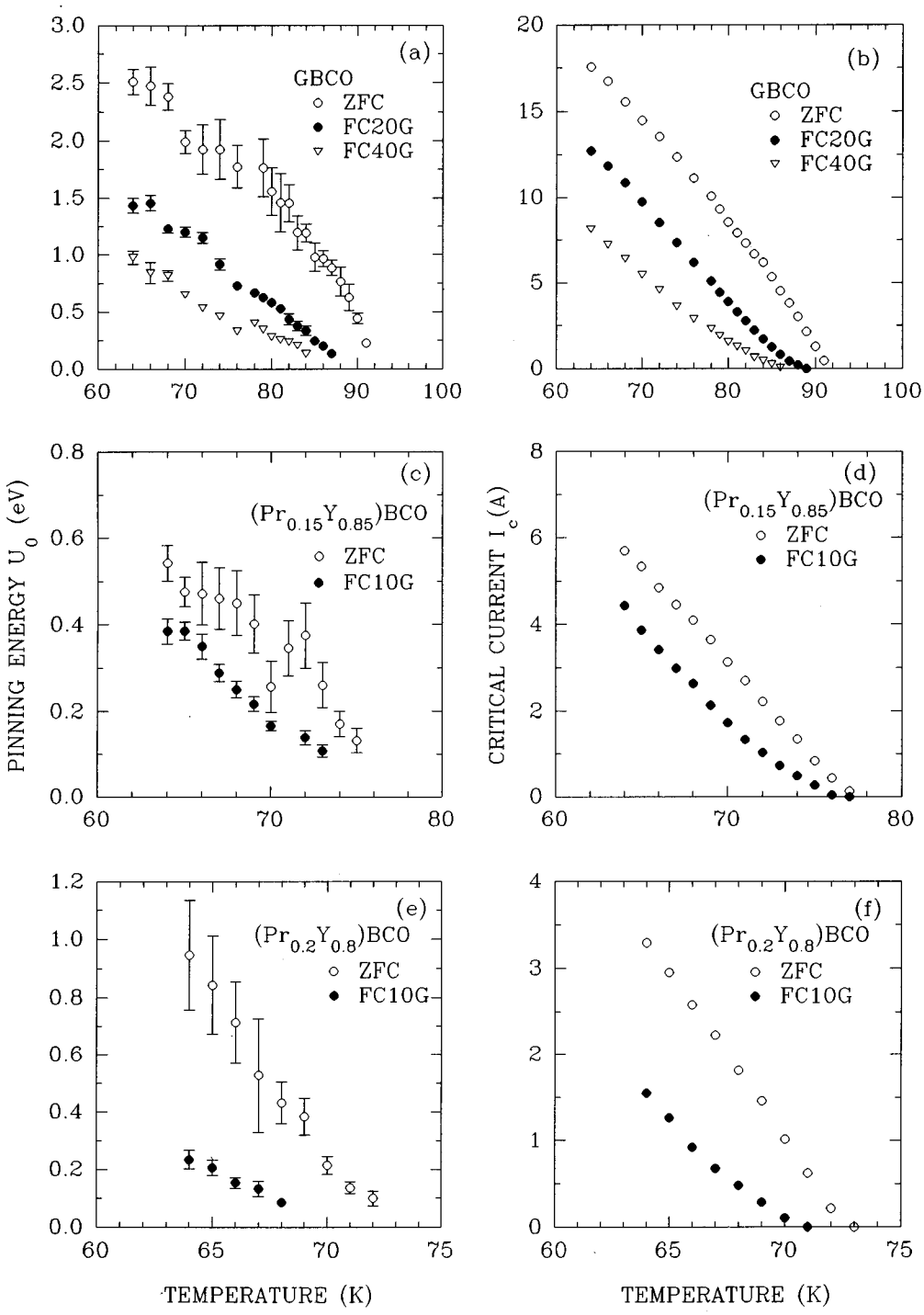

FIG. 4. Comparison of the temperature dependence of the unperturbed pinning potential $U_0(T,H)=kT/S(T,H)$ with that of the critical current $I_c(T,H)$ for granular GBCO and $(Pr_{0.15}Y_{0.85})BCO$ and $(Pr_{0.2}Y_{0.8})BCO$ samples. Note the similarities between the temperature dependence of $U_0(T,H)$ and that of $I_c(T,H)$.

effects in $I_c(T)$ exhibited by YBCO thin films and granular YBCO imply that the grains of granular YBCO are connected by microbridges of the grainlike material. These microbridges have the microdomain structure, and the intergrain critical current flowing through the microbridges experiences the AB→GL transition in the temperature dependence. An intergrain conduction through microbridges was proposed by Larbalestier *et al.*[24] in order to explain the field-independent residual intergrain critical current in ceramic high-temperature superconductors.

A microbridge model of electrical transport across the grain boundaries was adopted in order to describe the intergrain pinning and flux motion in granular high-T_c superconductors. One could visualize that the grain boundary contains a large number of parallel microbridges (filaments) in contact with each other, each carrying different critical current. In the AB regime, the microbridges can be described by a different effective Josephson coupling energy. This energy is determined by the Josephson junctions in the microdomain structure within a microbridge. In the GL regime, on the

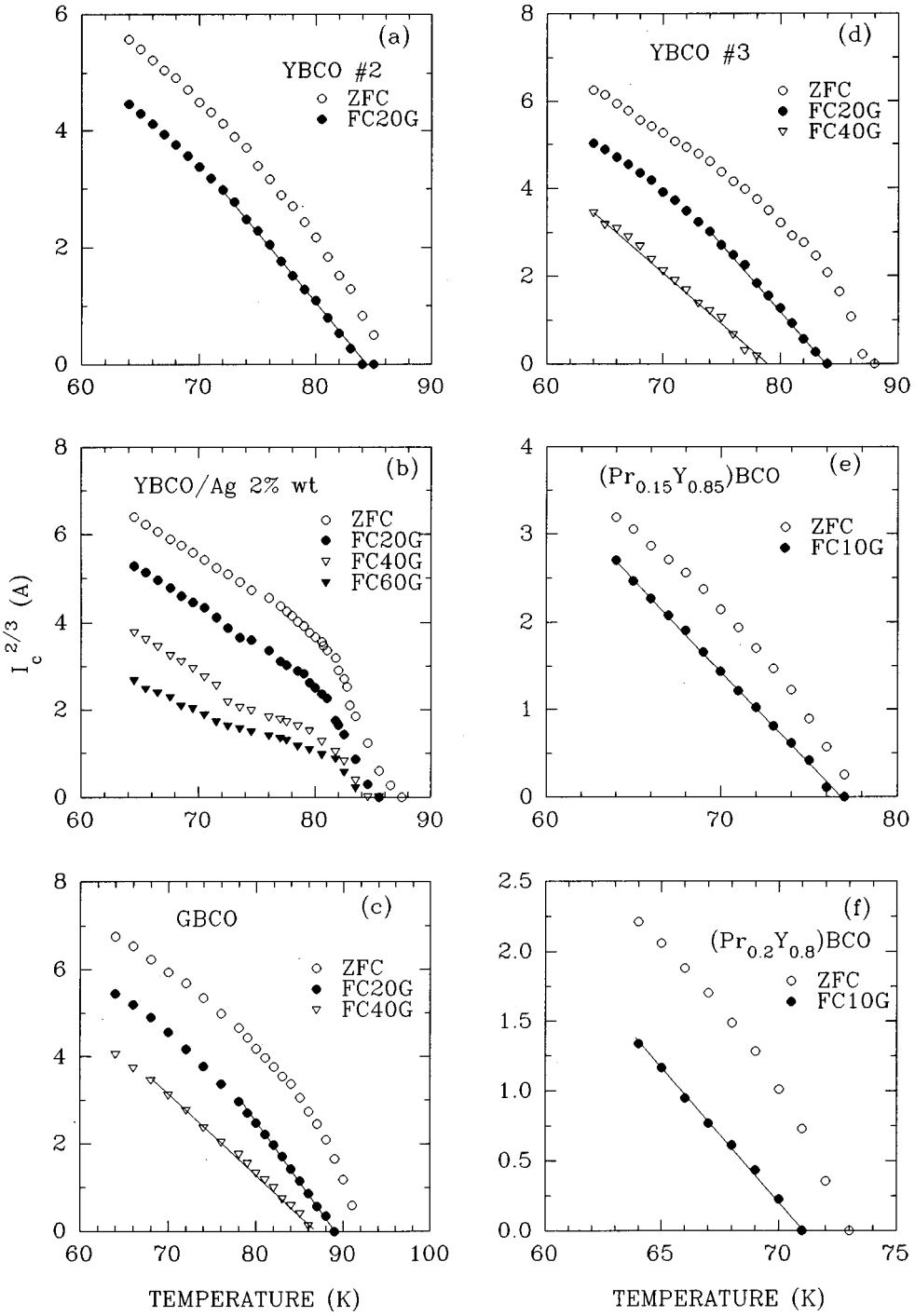

FIG. 5. $[I_c(T)]^{2/3}$ vs temperature plotted for the case of $I_c(T)$ which was measured in granular YBCO and *R*BCO samples [Figs. 1(d)–1(i)]. The transition from an Ambegaokar-Baratoff form of $I_c(T)$ to a Ginzburg-Landau one (solid lines) is observed for all samples [except YBCO/Ag (2 wt. %) in (b)] upon application of an increasing external magnetic field.

other hand, the microdomain structure is not ''seen'' by the supercurrent flowing through a microbridge. The microbridges are then characterized by different order parameters.

According to the Tinkham-Lobb model of inhomogeneous intergranular pinning, the pinning barrier U_0 in the AB regime arises from the variation of the Josephson coupling energy, $U_0=\delta(4E_J)\propto(T_c-T)$ close to T_c. In the GL regime the pinning barrier U_0 is determined by the variation of the order parameter, $U_0=\delta[(H_c^2/8\pi)(4\pi\xi^3)]\propto(T_c-T)^{1/2}$ since, close to T_c, H_c and ξ vary as (T_c-T) and as $(T_c-T)^{-1/2}$, respectively.[16]

Using the microbridge model, the absence of dissipation in some YBCO samples could be due to the separation of individual microbridges by normal regions. This could produce stronger pinning but limit the total intergrain critical current. This concept is supported by the fact that the critical

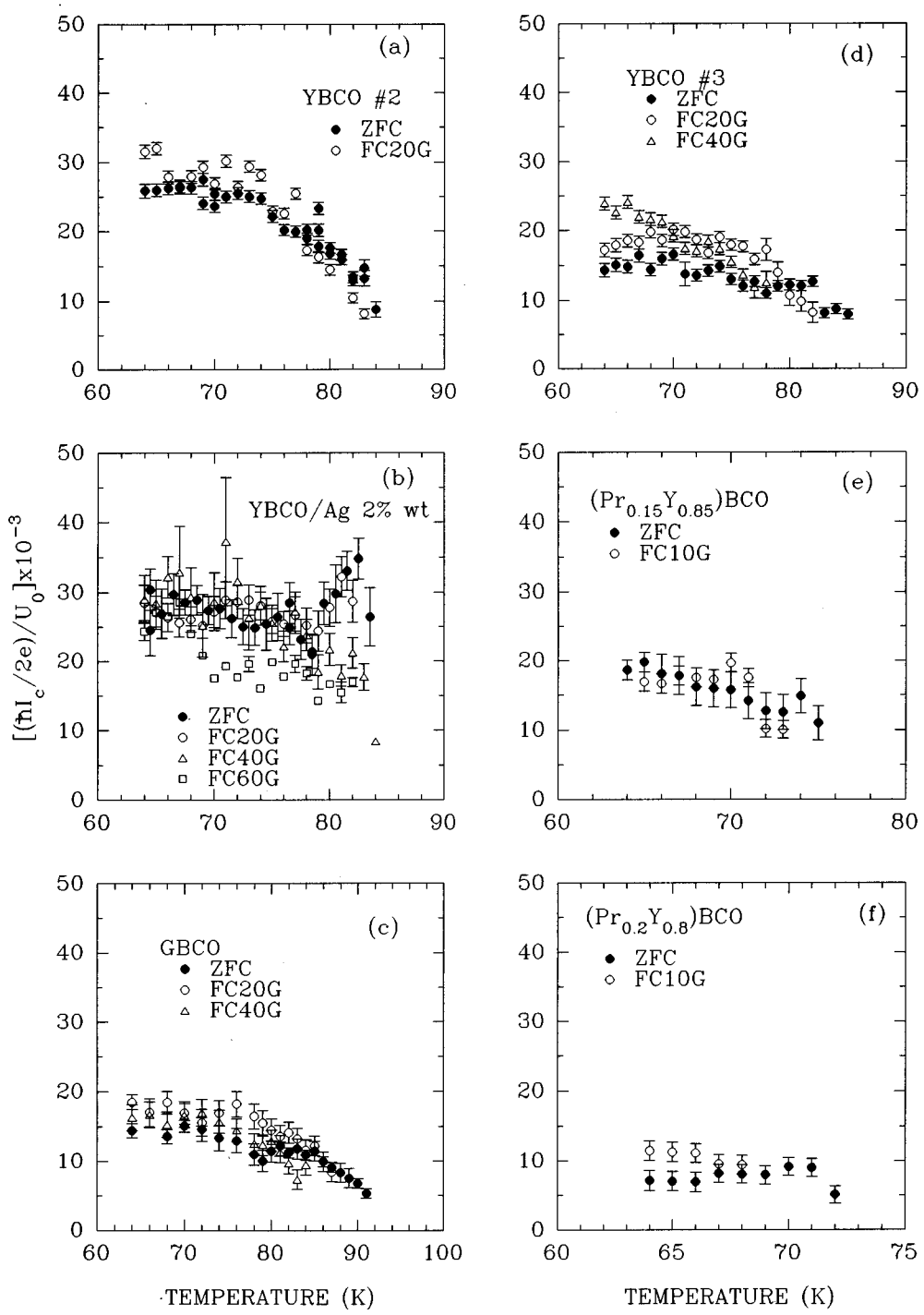

FIG. 6. Temperature dependence of the ratio $[\hbar I_c(T,H)/2e]/U_0(T,H)$ plotted for six different samples of YBCO and *R*BCO (R=Gd and Pr). Note that for all samples except YBCO/Ag the ratio decreases with an increasing temperature very close to T_c where the Ginzburg-Landau regime of $I_c(T)$ dominates.

current in YBCO No. 1 [Fig. 1(a)], which does not exhibit dissipation, is less than those in YBCO Nos. 2 and 3 [Figs. 1(d) and 1(g)].

In Fig. 6 we have plotted the ratio of the total coupling energy of junctions (summed over the ring's cross-sectional area) $E_J^*=\hbar I_c(T,H)/2e=\Sigma E_J(T,H)$ to the pinning barrier $U_0=kT/S(T,H)$ as a function of temperature. In the AB regime of $I_c(T)$, one expects $I_c\propto(T_c-T)$ close to T_c and $U_0=\delta(4E_J)\propto(T_c-T)$, leading to E_J^*/U_0, independent of temperature. In the GL regime, E_J^* does not have any physical meaning: therefore, E_J^*/U_0 has to be replaced by the ratio $(\text{const}\times I_c)/U_0$, where $I_c\propto(T_c-T)^{3/2}$ is a GL critical current and $U_0\propto(T_c-T)^{1/2}$. In this case the ratio $(\text{const}\times I_c)/U_0$ decreases with an increasing temperature as (T_c-T).

The ratio $[\hbar I_c(T,H)/2e]/U_0$ for YBCO Nos. 2 and 3 and for GBCO shows especially clearly the plateau at low temperatures where $I_c(T)$ is dominated by Josephson tunnel junctions and the decrease with an increasing temperature

close to T_c where $I_c(T)$ is the GL critical current. However, we have not attempted to fit the temperature dependence of U_0 [which is proportional to (T_c-T) in the AB regime and to $(T_c-T)^{1/2}$ in the GL regime close to T_c] to the experimental data shown in Figs. 3 and 4, due to the scattering of the data points.

The temperature dependence of the intergrain critical current in the zero-field-cooled YBCO/Ag (2 wt. %) composite was interpreted[21] as due to the Josephson *S-I-S* tunnel junctions [characterized by the AB form of $I_c(T)$] up to 80 K and by the Josephson *S-N-S* proximity junctions [with $I_c(T) \propto (T_c-T)^2$] above 80 K [Fig. 1(e)]. This could happen if oxygen-depleted superconducting layers (of $T_c \approx 80$ K) cross the intergrain microbridges. The external magnetic field converts $I_c(T)$ into a GL one close to T_c for all the samples studied except for YBCO/Ag (2 wt. %) (Fig. 5; see also Fig. 5 in Ref. 21). This implies that $I_c(T)$ close to T_c in YBCO/Ag (2 wt. %) is controlled by *S-N-S* junctions. *S-N-S* junctions could determine the variation of the Josephson coupling energy E_J in the intergrain microbridges and consequently the intergrain pinning potential.

V. SUMMARY AND CONCLUSIONS

We investigated the origin of the fast magnetic relaxation (diverging normalized logarithmic decay rate S) close to T_c in YBCO. We used granular ring-shaped high-T_c superconductors to study this phenomenon. The depinning critical currents in granular samples always exhibit fast decays with time (diverging S) close to T_c, which implies that the unperturbed pinning potential U_0 goes to zero at T_c. The temperature dependence of the critical current I_c exhibits a crossover from an AB dependence to a GL one, with the AB→GL crossover temperature decreasing with an increasing applied magnetic field. The decrease of U_0 with an increasing temperature was observed for both AB and GL regimes of $I_c(T)$, suggesting similar vortex pinning mechanism in these two cases.

These results were interpreted using the model of a granular superconductor whose grains are coupled by a large number of parallel microbridges. These microbridges can support different critical currents. In the AB regime, the microbridges are responsible for the variation of the Josephson coupling energy E_J along the grain boundaries. In the GL regime, however, the microbridges provide modulation of the order parameter. According to the Tinkham-Lobb description of the intergrain pinning in a granular superconductor due to random disorder, there is a conceptual equivalence of the pinning process in the AB (weakly linked) and GL (continuum) regimes. The pinning is provided by the variation of the Josephson coupling energy in the former case and by the variation of the order parameter in the latter one. In the AB regime, the pinning potential U_0 decreases with an increasing temperature as (T_c-T) close to T_c. In the GL regime, U_0 decreases as $(T_c-T)^{1/2}$ close to T_c. Therefore, at the AB→GL crossover temperature, there should be a conversion from the (T_c-T) dependence of U_0 at lower temperatures to the $(T_c-T)^{1/2}$ one close to T_c.

We believe that small variations in E_J or the order parameter at the grain boundaries of granular YBCO are responsible for the weak intergrain flux pinning and, consequently, for the dissipation of the critical current. In ceramic YBCO (with random orientation of the grains), the grain boundaries are predominantly high-angle ones. In melt-textured grain-aligned YBCO, the grains form low-angle grain boundaries. It was determined[25] that the low-angle grain boundaries provide strong flux pinning sites. Therefore the dissipation of the critical current is caused by the weaker intragrain flux pinning, with S and U_0 independent of temperature close to T_c.[18] Consequently, the divergence of S (and the reduction of U_0) with an increasing temperature close to T_c, observed in YBCO single crystals and epitaxial thin films, could stem from filamentary superconducting structures caused, for instance, by phase separation. Phase separation in YBCO single crystals has been investigated by Osofsky *et al.*[26] and Quadri *et al.*[27] These structures could have a similar effect on flux pinning as that of high-angle grain boundaries in granular YBCO.

ACKNOWLEDGMENTS

This work was supported by a grant from the National Sciences and Engineering Council of Canada (NSERC).

[1] M. Tinkham, *Introduction to Superconductivity*, 2nd ed. (McGraw-Hill, New York, 1996), p. 345.
[2] J. Halbritter, Phys. Rev. B **48**, 9735 (1993); M. Muroi and R. Street, Physica C **246**, 357 (1995).
[3] Y. Yeshurun, A. P. Malozemoff, and F. Holtzberg, J. Appl. Phys. **46**, 5797 (1988).
[4] D. A. Brawner, N. P. Ong, and Z. Z. Wang, Phys. Rev. B **47**, 1156 (1993).
[5] L. Civale, A. D. Marwick, M. W. McElfresh, T. K. Worthington, A. P. Malozemoff, F. H. Holtzberg, J. R. Thompson, and M. A. Kirk, Phys. Rev. B **65**, 1164 (1990).
[6] J. R. Thompson, Y. R. Sun, L. Civale, A. P. Malozemoff, M. W. McElfresh, A. D. Marwick, and F. H. Holtzberg, Phys. Rev. B **47**, 14 440 (1993).
[7] C. W. Hagen and R. Griessen, Phys. Rev. Lett. **62**, 2857 (1989).
[8] S. W. Goodyear, J. S. Satchell, R. G. Humphreys, N. G. Chew, and J. A. Edwards, Physica C **192**, 85 (1992).
[9] H. Darhmaoui, J. Jung, and M. W. McElfresh (unpublished).
[10] K. Enpuku, T. Kisu, R. Sako, K. Yoshida, M. Takeo, and K. Yamafuji, Jpn. J. Appl. Phys. **28**, L991 (1989).
[11] D. O. Welch, IEEE Trans. Magn. **MAG-27**, 1133 (1991).
[12] C. Keller, H. Kupfer, R. Meier-Hirmer, U. Wiech, V. Selvamanickam, and K. Salama, Cryogenics **30**, 410 (1990).
[13] C. Mee, A. I. M. Rae, W. F. Vinen, and C. E. Gough, Phys. Rev. B **43**, 2946 (1991).
[14] J. Jung, I. Isaac, and M. A-K. Mohamed, Phys. Rev. B **48**, 7526 (1993).
[15] L. M. Paulius, C. C. Almasan, and M. B. Maple, Phys. Rev. B **47**, 11 627 (1993).
[16] P. J. Kung, M. P. Maley, M. E. McHenry, J. O. Willis, J. Y.

Coulter, M. Murakami, and S. Tanaka, Phys. Rev. B **46**, 6427 (1992).
[17] M. Tinkham and C. J. Lobb, Solid State Phys. **42**, 91 (1989).
[18] I. Isaac, J. Jung, M. Murakami, S. Tanaka, M. A-K. Mohamed, and L. Friedrich, Phys. Rev. B **51**, 11 806 (1995).
[19] C. J. Lobb, D. W. Abraham, and M. Tinkham, Phys. Rev. B **27**, 150 (1983).
[20] M. Tinkham, D. W. Abraham, and C. J. Lobb, Phys. Rev. B **28**, 6578 (1983).
[21] H. Darhmaoui and J. Jung, Phys. Rev. B **53**, 14 621 (1996).
[22] J. R. Clem, B. Bumble, S. I. Raider, W. J. Gallagher, and Y. C. Shih, Phys. Rev. B **35**, 6637 (1987).
[23] J. Etheridge, Philos. Mag. A **73**, 643 (1996).
[24] D. C. Larbalestier, S. E. Babcock, X. Cai, L. Cooley, M. Daeumling, D. P. Hampshire, J. McKinnel, and J. Seuntjens, in *Progress in High Temperature Superconductivity*, edited by S. Nakajima (World Scientific, Englewood Cliffs, NJ, 1989), Vol. 18, p. 128.
[25] M. Turchinskaya, D. L. Kaiser, F. W. Gayle, A. J. Shapiro, A. Roytburd, L. A. Dorosinskii, V. I. Nikitenko, A. A. Polyanskii, and V. K. Vlasko-Vlasov, Physica C **221**, 62 (1994).
[26] M. S. Osofsky, J. L. Cohn, E. F. Skelton, M. M. Miller, R. J. Soulen, Jr., and S. A. Wolf, Phys. Rev. B **45**, 4916 (1992).
[27] S. B. Quadri, M. S. Osofsky, V. M. Browning, and E. F. Skelton, Appl. Phys. Lett. **68**, 2729 (1996).